Int J Clin Exp Pathol 2015;8(12):15863-15870
www.ijcep.com /ISSN:1936-2625/IJCEP0010569

Original Article

Effect of halofuginone on the inhibition of proliferation and invasion of hepatocellular carcinoma HepG2 cell line

Sibo Huo[1], Huiqiu Yu[1], Chusheng Li[1], Jiayu Zhang[1], Tongjun Liu[2]

[1]Department of Pharmacy, China-Japan Union Hospital, Jilin University, Changchun 130033 China; [2]Colorectal and Anal Surgery, China-Japan Union Hospital, Jilin University, Changchun 130033, China

Received May 23, 2015; Accepted June 28, 2015; Epub December 1, 2015; Published December 15, 2015

Abstract: Primary liver cancer is a common cancer and the mortality of liver cancer ranks the second of all malignancy-related deaths in China. The most common primary liver cancer is hepatocellular carcinoma, accounting for approximately 90% of the total. Because liver is the largest parenchymatous organ in the body undertaking all kinds of important metabolic functions, liver cancer inevitably causes greater harms and its treatment is extremely difficult. Currently, there are still no effective drugs for the treatment of patients with advanced inoperable liver cancer. We observed the strong inhibitory activity of halofuginone on HepG2 cell growth and the cell cycle and apoptosis assays showed that halofuginone arrested the cell cycle and inhibited the induction. And we found that halofuginone inhibits tumor cell cycle possibly by up-regulating p15 and p21 of expression. Then, we found that the proportion of cleaved PARP, caspase-3, 8 and 9 in HepG2 cells increased after halofuginone treatment. And the results showed that halofuginone down-regulated Mcl-1 and c-IAP1 expression. Finally, our results showed halofuginone regulated the activities of JNK and MEK/ERK signaling pathways in hepatocellular carcinoma cells. In summary, this study shows that halofuginone can inhibit the in vitro growth, arrest the cell cycle and induce the apoptosis of HepG2 cells. Its mechanisms of action may be related to the regulation of associated protein expression, up-regulation of JNK, and inhibition of MEK/ERK signaling pathway.

Keywords: Halofuginone, hepatocellular carcinoma, proliferation, invasion

Introduction

Primary liver cancer is a common cancer; the mortality of primary liver cancer ranks the second of all malignancy-related deaths in China [1]. The most common primary liver cancer is hepatocellular carcinoma, accounting for approximately 90% of the total [2]. Because liver is the largest parenchymatous organ in the body undertaking all kinds of important metabolic functions, liver cancer inevitably causes greater harms. In addition, the liver has rich blood supply and close relationship with other organs of the digestive system, its treatment is extremely difficult. Currently, there are still no effective drugs for the treatment of patients with advanced inoperable liver cancer [3].

Dichroa fabrifuga is a traditional Chinese medicine that has been used in China for hundreds of years with significant anti-malarial efficacy. Halofuginone is a halogenated derivative of febrifugine, which is the main active ingredient of dichroa fabrifuga. Halofuginone can not only increase the drug efficacy but also reduce the gastrointestinal toxicity of febrifugine at the same time [4]. Studies have found that halofuginone has extensive and extremely significant anti-tumor effect. Currently, it has been found that halofuginone can suppress a variety of cancers including bladder cancer, liver cancer, melanoma, breast cancer and leukemia [5-10]. Although it was reported that halofuginone could inhibit the in vitro and in vivo growth of hepatocellular carcinoma Hep3B cell line as early as in 2004, the subsequent studies are few and its mechanism of liver cancer suppression is yet to be determined. This study mainly investigated the inhibitory effect of halofuginone on hepatocellular carcinoma HepG2 cell line and preliminarily explored its molecular mechanisms of action.

Material and methods

Cell culture

The cells were cultured in an incubator under 37°C, 5% CO_2 and saturated humidity condition. The culture medium was DMEM supplemented with 10% FBS. The cells were digested with 0.25% trypsin-EDTA for passaging. Cells in logarithmic growth phase were used in all experiments.

MTS cell growth assay

The cells in logarithmic growth phase, 8×10^4 cells/ml, were seeded in 96-well microplates, 100 μl/well, and cultured overnight to allow cell adherence. Then, different concentrations of halofuginone were added to continue the culture for 72 h. Then, the medium was removed and MTS was added in accordance with the reagent instructions to continue the culture for 4 h. Finally, the OD value was measured at 490 nm wavelength with a microplate reader to represent the cell counts. The inhibition rate of this drug on cells was calculated as follows: inhibition rate = (1-experimental group OD/control group OD) × 100%.

Cell cycle and apoptosis assay

The cell cycle was determined with PI staining technique. After treatment with 100 or 200 nM halofuginone for 24 h, the cells were collected using method described in the instructions to determine the cell cycle. Cell apoptosis was determined with Annexin V-FITC/PI double-staining technique. After treatment with 100 or 200 nM halofuginone for 24 h, the cells were collected using method described in the instructions to determine the apoptosis.

Cell invasion assay

In vitro invasive assays were performed using the Millicell Cell Culture. Matrigel was added to the filter and allowed to set for 5 h at 37°C. Cancer cells were harvested centrifuged and re-suspended to form single-cell suspension. Thereafter, 1×10^5 cells per well were seeded into the invasion assay insert. The lower compartment of the chamber was filled with DMEM plus 20% FBS. After 24-hour incubation, the transwell inserts were removed from the plate and the cells that migrated to the lower surface of the filter were fixed with the methanol and stained with crystal violet for 30 min and then dissolved with 33% acetic acid. The cells were photographed and the numbers of cells were indirectly quantitated by measuring the absorbance at 570 nm. Each assay was done in triplicate and repeated at least thrice. The data were analyzed using student's t test and the statistical significance was set at $P < 0.05$.

Wound-healing assay

Cells in exponential growth phase were grown in 24-well plates until they reached confluence. We scraped 3 horizontal lines across the entire diameter at the bottom of each well inducing the "wound". Cell media was removed and the cells were gently rinsed 3 times to remove unattached cells. The wound area was photographed at 24 h after scraping. To compare cell motility of cancer cells, we measured the gap distance and determined the wound-closing rate. The cells were allowed to migrate into the wounded area for 24 h. At the indicated time points, the wound closure was photographed by a camera attached to an inverted microscope.

Western blotting assay

After treatment with halofuginone, the cells were lysed to extract the proteins from the lysate. The proteins were separated in 12% SDS-PAGE and then transferred to a PVDF membrane; the target proteins were detected with different antibodies (4°C overnight). After washing off the primary antibodies, the membrane was incubated with HRP-conjugated secondary antibody for 1 h; ECL kit was used to develop the immunoreactive bands. Then β-actin was used as an internal control to determine the changes in MMP2, MMP9, MMP14, CD44, E-cadherin, p15, p21, Mcl-1 and c-IAP1 expression levels, cleaved PARP, caspases-3, 8 and 9 levels, and JNK and p38MAPK phosphorylation levels in these cells.

Real-time PCR assay

Total RNA was extracted from each group using Trizol method. Real-Time PCR Kit was used to carry out reverse transcription to obtain the cDNA; then, MMP2, MMP9, MMP14, CD44, E-cadherin, p15, p21, Mcl-1 and c-IAP1 mRNA levels were detected. The transcription level of target proteins was detected by semiquantita-

Table 1. Oligonucleotide sequences used for real-time PCR

Gene	Primer sequences (5'-3')
MMP2	Forward: TACTGAGTGGCCGTGTTTGC
	Reserse: AGGGAGCAGAGATTCGGACTT
MMP9	Forward: GGGCTTAGATCATTCCTCAGTG
	Reserse: GCCATTCACGTCGTCCTTAT
MMP14	Forward: TGCCTGCGTCCATCAACA
	Reserse: ATCTTGTCGGTAGGCAGC
E-cadherin	Forward: AGAACGCATTGCCACATACACTC
	Reverse: CATTCTGATCGGTTACCGTGATC
CD44	Forward: TATGACACATATTGCTTCAATGC
	Reverse: GTGTACCATCACGGTTGACA
p15	Forward: AAGCTGAGCCCAGGTCTCCTA
	Reverse: CCACCGTTGGCCGTAAACT
p21	Forward: CACTCCAAACGCCGGCTGATCTTC
	Reverse: TGTAGAGCGGGCCTTTGAGGCCCTC
Mcl-1	Forward: GGGCAGGATTGTGACTCTCATT
	Reverse: GATGCAGCTTTCTTGGTTTATGG
c-IAP1	Forward: AGCTAGTCTGGGATCCACCTC
	Reverse: GGGGTTAGTCCTCGATGAAG
GAPDH	Forward: CTTAGATTTGGTCGTATTGG
	Reverse: GAAGATGGTGATGGGATT

tive real-time PCR using the cycler IQ detection system (Bio-Rad). The PCR condition was as following: decontamination at 50°C for 2 min, denaturation at 95°C for 2 min, followed by 40 cycles at 95°C for 20 seconds and at hybridization 72°C for 40 seconds. Expression levels of genes were normalized to that of the housekeeping gene GAPDH as the control. The full details of primers were shown in **Table 1**.

Statistical analysis

Experimental data were expressed as mean ± standard deviation; SPSS13.0 software was used for analysis. One-way ANOVA was carried out for comparison; $P < 0.05$ indicated statistically significant differences.

Results

Halofuginone inhibits proliferation, arrests cells in G0/G1 phase and promotes apoptosis of HepG2 cells in vitro

MTS cell proliferation assay showed that halofuginone inhibited the in vitro proliferation of HepG2 cells, with an IC50 of 72.7 nM for 72 h (**Figure 1A**). The results showed that the proportion of cells in G0/G1 phase increased in dose-dependent manner after treatment for 24 h, as shown in **Figure 1B** and **1C**. In addition, the apoptosis ratio significantly increased after treatment for with 100 and 200 nM halofuginone for 24 h in dose-dependent manner, as shown in **Figure 1D** and **1E**.

Halofuginone up-regulates intracellular p15 and p21 expression

In the meantime with cell cycle analysis, we used WB to determine the intracellular expression levels of p15 and p21 proteins that negatively regulate the cell cycle. The results showed that, when compared with the control group, E-cadherin, p15 and p21 expression levels were significantly up-regulated in halofuginone-treated tumor cells. But the protein expressions of MMP2, MMP9, MMP14 and CD44 in halofuginone-treated tumor cells were significantly down-regulated (**Figure 2B**). The RT-PCR results showed that this regulation may occur at transcriptional level, as shown in **Figure 2A**, and the results of RT-PCR were consistent with the results of western blot. A key feature of cells that have higher MMPs expression is their increased migration and invasion capacity. The results of the cell invasion (**Figure 2D**) and the wound-healing assay (**Figure 2C**) showed that the metastatic capacity of cells was inhibited by halofuginone. The amount of cells that migrated to the lower side of the membrane was significantly reduced and the migration of cells was also prominently decreased after transfected with halofuginone (**Figure 2E**).

Halofuginone enhances the cleavage of PARP, caspases-3, 8 and 9, and down-regulates Mcl-1 and c-IAP1 expression

In addition to apoptosis assay, we used western blot to determine the intracellular expression of apoptosis-related proteins. The results showed that, when compared with the control group, PARP, caspases-3, 8 and 9 cleavage product levels increased in HepG2 cells after treatment with halofuginone, as shown in **Figure 3A**, suggesting activation of the caspase apoptosis pathway. Meanwhile, the expression of Mcl-1 and c-IAP1 proteins inhibiting apoptosis was down-regulated, as shown in **Figure 3C**. RT-PCR results showed that the regulation of halofuginone on Mcl-1 and c-IAP1 may occur at transcriptional level, as shown in **Figure 3B**.

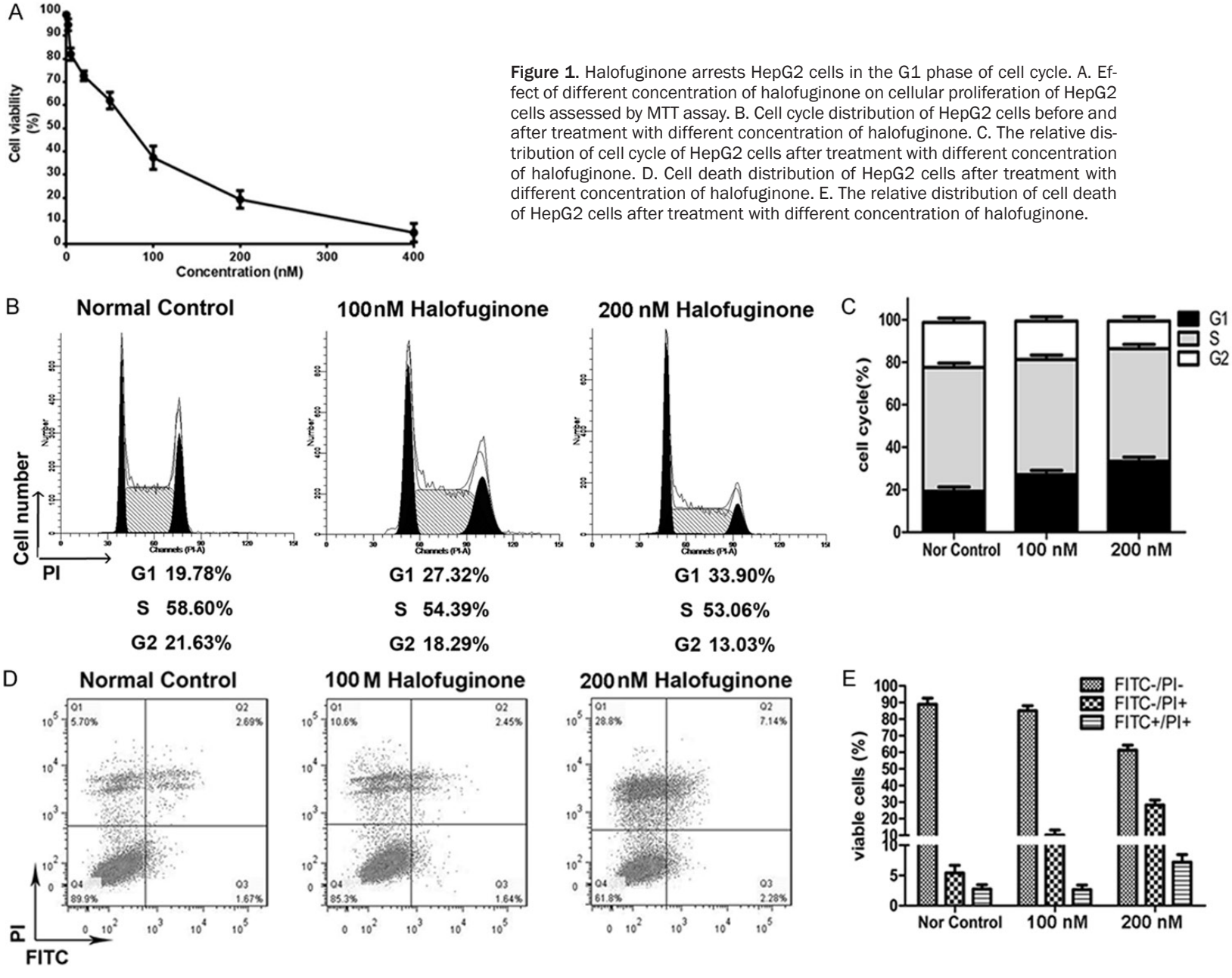

Figure 1. Halofuginone arrests HepG2 cells in the G1 phase of cell cycle. A. Effect of different concentration of halofuginone on cellular proliferation of HepG2 cells assessed by MTT assay. B. Cell cycle distribution of HepG2 cells before and after treatment with different concentration of halofuginone. C. The relative distribution of cell cycle of HepG2 cells after treatment with different concentration of halofuginone. D. Cell death distribution of HepG2 cells after treatment with different concentration of halofuginone. E. The relative distribution of cell death of HepG2 cells after treatment with different concentration of halofuginone.

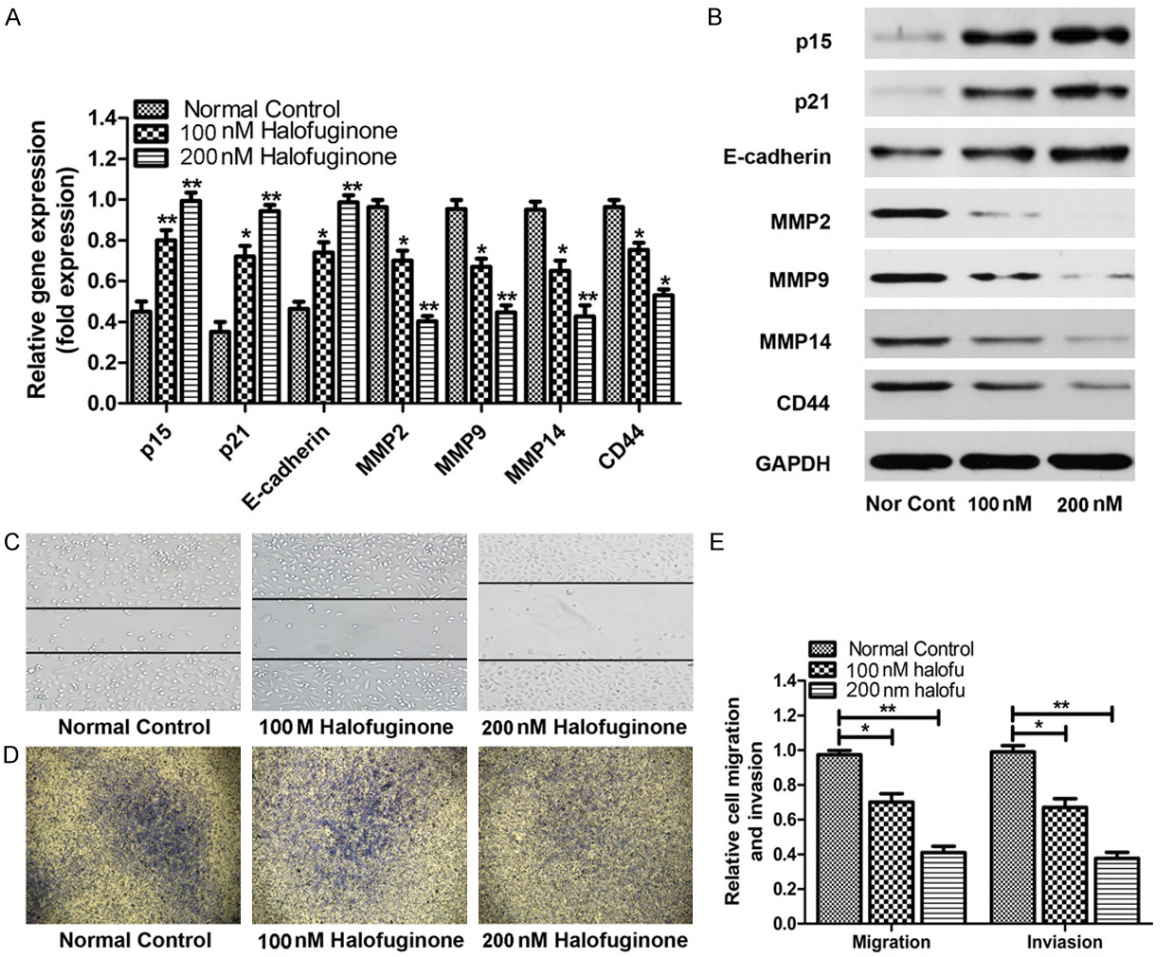

Figure 2. Halofuginone inhibits the metastasis of HepG2 cells. A, B. Detection of p15, p21, E-cadherin, MMP2, MMP9, MMP14 and CD44 gene/protein expressions in HepG2 cells after treatment with different concentration of halofuginone. C. Representative pictures of wound-healing assay for cell migration after treatment with different concentration of halofuginone. D. Representative images of transwell assay for cell invasion after CD44 interference. E. The relative cells migration and invasion. *P < 0.05, **P < 0.01, compared with the control.

Halofuginone up-regulates JNK phosphorylation and down-regulates p38MAPK phosphorylation

Furthermore, we used western blot to determine the activity levels of JNK and MEK/ERK signaling pathways. The results showed that halofuginone significantly up-regulated JNK phosphorylation, suggesting increased activity of JNK pathway. Meanwhile, halofuginone significantly inhibited p38MAPK phosphorylation level, suggesting inhibition of the activity of MEK/ERK signaling pathway. The details were shown in **Figure 4**.

Discussion

In MTS assay, we observed the strong inhibitory activity of halofuginone on HepG2 cell growth; while cell cycle and apoptosis assays showed that halofuginone arrested the cell cycle and inhibited the induction. These results strongly suggested that halofuginone has anti-HepG2 effect. Nagler *et al* [11]. Observed similar results in another hepatocellular carcinoma Hep3B cell line [11].

In cell cycle assay, we observed that halofuginone arrested the cell cycle in G0/G1 phase. To investigate the mechanism that halofuginone blocks the cell cycle, we used WB to determine p15 and p21 expression levels; the results showed that halofuginone up-regulated p15 and p21 of expression. Both p15 and p21 are negative cell cycle regulatory proteins; p15 can selectively inhibit CDK4/6 activity while p21 is a cell cycle kinase essential for G1 phase [12]. Due to its ability to inhibit CDK2, CDK1 and

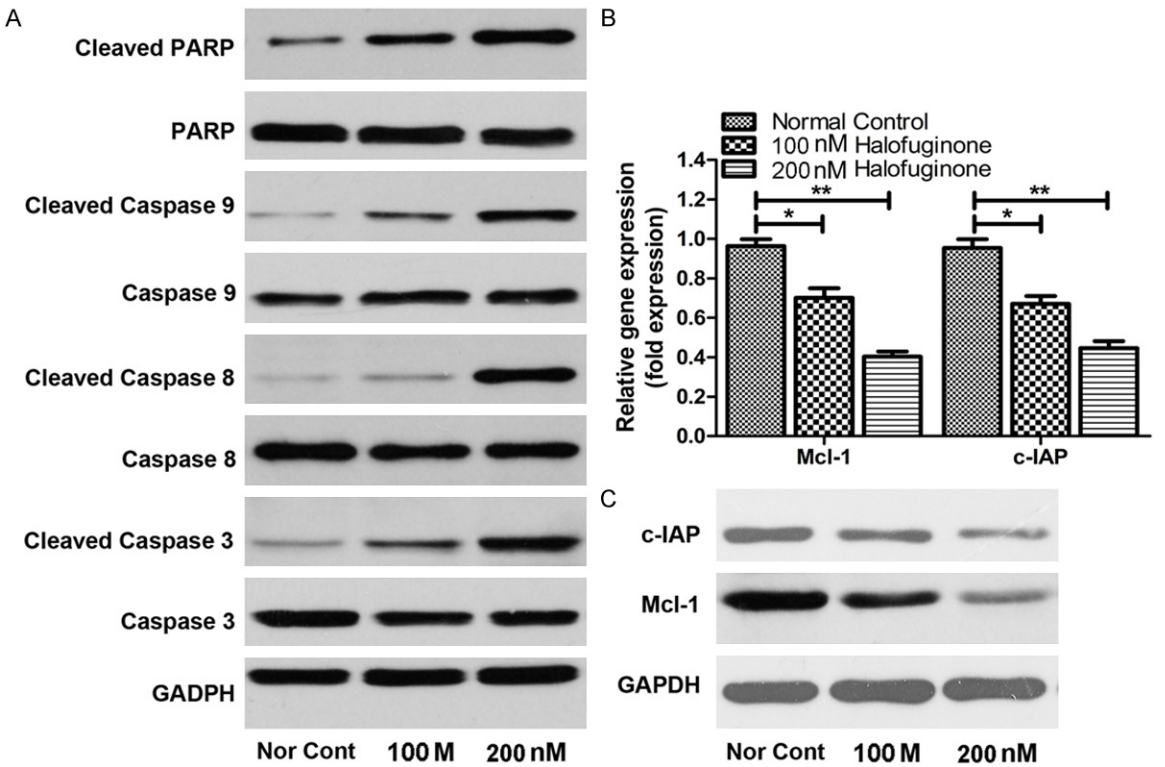

Figure 3. Halofuginone down-regulates the expressions of Mcl-1 and c-IAP in HepG2 cells. A. The increased protein expressions of cleaved PARP, caspase 3, caspase 8 and caspase 9 in HepG2 after treatment with different concentration of halofuginone. B, C. Detection of Mcl-1 and c-IAP gene/protein expressions in HepG2 cells after treatment with different concentration of halofuginone.

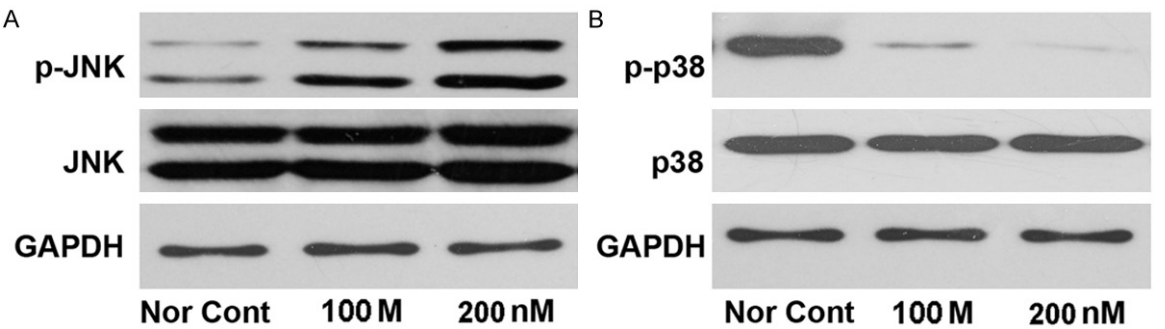

Figure 4. MAPK signaling pathway involves in halofuginone-mediated inhibition of HepG2 cells. A. The increased protein expressions of p-JNK in HepG2 after treatment with different concentration of halofuginone. B. The decreased protein expressions of p-p38 in HepG2 after treatment with different concentration of halofuginone.

CDK4/6 activity, p21 has broader actions and is able to arrest the cells in G1 and S phase [13]. These results suggest that halofuginone inhibits tumor cell cycle possibly by up-regulating p15 and p21 of expression.

After having observed that halofuginone significantly induced HepG2 apoptosis, we further analyzed its molecular mechanism. A recent study showed that halofuginone was able to activate caspase pathway to induce tumor apoptosis. We detected several major proteins in caspase pathway, including PARP, caspase-3, 8 and 9, which often produce cleaved active products through the action of upstream proteases [14]. WB assay showed that the proportion of cleaved PARP, caspase-3, 8 and 9 in HepG2 cells increased after halofuginone treat-

ment, which confirmed our speculation. We also determined two other anti-apoptosis proteins, Mcl-1 [15, 16] and c-IAP1 [17], in hepatocellular carcinoma cells. Mcl-1 and c-IAP1 are also closely related to caspase signaling pathway; Mcl-1 is a substrate for caspase-3 while c-IAP1 can inhibit caspase-8 activity to exert its actions [18]. WB assay showed that halofuginone down-regulated Mcl-1 and c-IAP1 expression.

Finally, we explored how halofuginone regulated hepatocellular carcinoma-related key signaling pathways. A recent study showed that halofuginone was able to regulate the activities of JNK and MEK/ERK signaling pathways [19]. In liver cancer, JNK plays dual roles: on one hand, it facilitates inflammation in hepatic microenvironment to support tumor progression, on the other hand, it acts on the hepatocytes to suppress tumor growth [20]. This study showed that halofuginone increased JNK phosphorylation level in hepatocellular carcinoma cells, indicating an elevated activity of the JNK signaling pathway; this suggests that tumor suppression is the main effect after halofuginone has up-regulated JNK activity. MEK/ERK signaling pathway plays an important role in the progression of hepatocellular carcinoma; one of the main mechanisms of sorafenib action, which is a targeted drug for the treatment of hepatocellular carcinoma, is to inhibit this signaling pathway [21]. Our study showed that halofuginone was also able to inhibit the activity of this signaling pathway.

In summary, this study shows that halofuginone can inhibit the in vitro growth, arrest the cell cycle and induce the apoptosis of HepG2 cells. Its mechanisms of action may be related to the regulation of associated protein expression, up-regulation of JNK, and inhibition of MEK/ERK signaling pathway.

Disclosure of conflict of interest

None.

Address correspondence to: Dr. Tongjun Liu, Colorectal and Anal Surgery, China-Japan Union Hospital of Jilin University, Changchun 130033, China. E-mail: tongjun_liuzr@126.com

References

[1] Gao J, Xie L, Chen WQ, Zhang SW, Wu QJ, Yang Y, Yang WS, Tan YT, Xiang YB. Rural-urban, sex variations, and time trend of primary liver cancer incidence in China, 1988-2005. Eur J Cancer Prev 2013; 22: 448-454.

[2] Giuliani J, Marzola M, Pansini G. Liver metastases from primary rectal cancer: a multidisciplinary reverse approach. J Gastrointest Cancer 2013; 44: 368-369.

[3] Qi JS, Wang WH, Li FQ. Combination of interventional adenovirus-p53 introduction and ultrasonic irradiation in the treatment of liver cancer. Oncol Lett 2015; 3: 1297-1302.

[4] McLaughlin NP, Evans P, Pines M. The chemistry and biology of febrifugine and halofuginone. Bioorg Med Chem 2014; 7: 1993-2004.

[5] Chu TL, Guan Q, Nguan CY, Du C. Halofuginone suppresses T cell proliferation by blocking proline uptake and inducing cell apoptosis. Int Immunopharmacol 2013; 16: 414-423.

[6] de Figueiredo-Pontes LL, Assis PA, Santana-Lemos BA, Jácomo RH, Lima AS, Garcia AB, Thomé CH, Araújo AG, Panepucci RA, Zago MA, Nagler A, Falcão RP, Rego EM. Halofuginone has anti-proliferative effects in acute promyelocytic leukemia by modulating the transforming growth factor beta signaling pathway. PLoS One 2011; 6: e26713.

[7] Jin ML, Park SY, Kim YH, Park G, Lee SJ. Halofuginone induces the apoptosis of breast cancer cells and inhibits migration via down-regulation of matrix metalloproteinase-9. Int J Oncol 2014; 44: 309-318.

[8] Juárez P, Mohammad KS, Yin JJ, Fournier PG, McKenna RC, Davis HW, Peng XH, Niewolna M, Javelaud D, Chirgwin JM, Mauviel A, Guise TA. Halofuginone inhibits the establishment and progression of melanoma bone metastases. Cancer Res 2012; 72: 6247-6256.

[9] Liang J, Zhang B, Shen RW, Liu JB, Gao MH, Geng X, Li Y, Li YY, Zhang W. The effect of anti-fibrotic drug halofugine on Th17 cells in concanavalin A-induced liver fibrosis. Scand J Immunol 2014; 3: 163-72.

[10] Machado SA, Bahr JM, Hales DB, Braundmeier AG, Quade BJ, Nowak RA. Validation of the aging hen (Gallus gallus domesticus) as an animal model for uterine leiomyomas. Biol Reprod 2014; 87: 86.

[11] Nagler A, Ohana M, Shibolet O, Shapira MY, Alper R, Vlodavsky I, Pines M, Ilan Y. Suppression of hepatocellular carcinoma growth in mice by the alkaloid coccidiostat halofuginone. Eur J Cancer 2004; 40: 1397-1403.

[12] Inoue S, Hao Z, Elia AJ, Cescon D, Zhou L, Silvester J, Snow B, Harris IS, Sasaki M, Li WY, Itsumi M, Yamamoto K, Ueda T, Dominguez-Brauer C, Gorrini C, Chio II, Haight J, You-Ten A, McCracken S, Wakeham A, Ghazarian D, Penn LJ, Melino G, Mak TW. Mule/Huwe1/Arf-BP1 suppresses Ras-driven tumorigenesis by pre-

venting c-Myc/Miz1-mediated down-regulation of p21 and p15. Genes Dev 2013; 27: 1101-1114.

[13] Zhao H, Zhang S, Xu D, Lee MY, Zhang Z, Lee EY, Darzynkiewicz Z. Expression of the p12 subunit of human DNA polymerase delta (Pol delta), CDK inhibitor p21 (WAF1), Cdt1, cyclin A, PCNA and Ki-67 in relation to DNA replication in individual cells. Cell Cycle 2014; 13: 3529-3540.

[14] Zheng B, Chai R, Yu X. Downregulation of NIT2 inhibits colon cancer cell proliferation and induces cell cycle arrest through the caspase-3 and PARP pathways. Int J Mol Med 2015; 5: 1317-22.

[15] Leverson JD, Zhang H, Chen J, Tahir SK, Phillips DC, Xue J, Nimmer P, Jin S, Smith M, Xiao Y, Kovar P, Tanaka A, Bruncko M, Sheppard GS, Wang L, Gierke S, Kategaya L, Anderson DJ, Wong C, Eastham-Anderson J, Ludlam MJ, Sampath D, Fairbrother WJ, Wertz I, Rosenberg SH, Tse C, Elmore SW, Souers AJ. Potent and selective small-molecule MCL-1 inhibitors demonstrate on-target cancer cell killing activity as single agents and in combination with ABT-263 (navitoclax). Cell Death Dis 2015; 6: e1590.

[16] Modugno M, Banfi P, Gasparri F, Borzilleri R, Carter P, Cornelius L, Gottardis M, Lee V, Mapelli C, Naglich JG, Tebben A, Vite G, Pastori W, Albanese C, Corti E, Ballinari D, Galvani A. Mcl-1 antagonism is a potential therapeutic strategy in a subset of solid cancers. Exp Cell Res 2015; 2: 267-77.

[17] Xu W, Liu L, Hornby D. c-IAP1 binds and processes PCSK9 protein: linking the c-IAP1 in a TNF-alpha pathway to PCSK9-mediated LDLR degradation pathway. Molecules 2002; 17: 12086-12101.

[18] Wong JC, Bathina M, Fiscus RR. Cyclic GMP/protein kinase G type-Iα (PKG-Iα) signaling pathway promotes CREB phosphorylation and maintains higher c-IAP1, livin, survivin, and Mcl-1 expression and the inhibition of PKG-Iα kinase activity synergizes with cisplatin in non-small cell lung cancer cells. J Cell Biochem 2012; 11: 3587-98.

[19] Roffe S, Hagai Y, Pines M, Halevy O. Halofuginone inhibits Smad3 phosphorylation via the PI3K/Akt and MAPK/ERK pathways in muscle cells: effect on myotube fusion. Exp Cell Res 2010; 6: 1061-9.

[20] Zheng Z, Tan C, Xiang G, Mai G, Liu X. Deleted in liver cancer-1 inhibits cell growth and tumorigenicity in human pancreatic cancer. Oncol Lett 2013; 2: 521-524.

[21] Thabut D, Routray C, Lomberk G, Shergill U, Glaser K, Huebert R, Patel L, Masyuk T, Blechacz B, Vercnocke A, Ritman E, Ehman R, Urrutia R, Shah V. Complementary vascular and matrix regulatory pathways underlie the beneficial mechanism of action of sorafenib in liver fibrosis. Hepatology 2011; 54: 573-585.